

# Structure, formation and decay of $\bar{K}NN$ system by Faddeev-AGS calculations

S. Marri and S. Z. Kalantari

*Department of Physics, Isfahan University of Technology, Isfahan 84156-83111, Iran*

J. Esmaili

*Department of Physics, Faculty of Basic Sciences,  
Shahrekord University, Shahrekord, 115, Iran*

(Dated: March 19, 2019)

## Abstract

The Faddeev AGS equations are solved for coupled-channels  $\bar{K}NN - \pi\Sigma N$  system with quantum numbers  $I = 1/2$  and  $S = 0$ . Using separable potentials for  $\bar{K}N - \pi\Sigma$  interaction, we have calculated the transition probability for the  $(Y_K)_{I=0} + N \rightarrow \pi\Sigma N$  reaction. The possibility to observe the trace of  $K^-pp$  quasi-bound state in the  $\pi\Sigma N$  mass spectra was studied. Various types of chiral based and phenomenological potentials are used to describe the  $\bar{K}N - \pi\Sigma$  interaction. It was shown that not only we can see the signature of the  $K^-pp$  quasi-bound state in the mass spectra, but also, one can see the trace of branch points in the observables.

PACS numbers: 13.75.Jz, 14.20.Pt, 21.85.+d, 25.80.Nv

## I. INTRODUCTION

The wish to define a precise interaction model for  $\bar{K}N$  interaction is a basic goal in strangeness nuclear physics. For the past two decades, an enormous amount of efforts has been made to study the structure of dense kaonic nuclear clusters [1–4]. An important kaonic cluster is the  $K^-pp$  system, which is a highly controversial issue in studying the kaonic systems. Many theoretical calculations were performed, focusing on the  $K^-pp$  system [5–15]. All few-body calculations have shown that the  $K^-pp$  is bound, but with some variation in the values of the extracted pole energy.

If  $K^-pp$  system is indeed bound, then the remaining question is whether this state is sufficiently narrow to allow observation and identification. Due to strong absorption of antikaon by the nucleus, the quasi-bound state in  $\bar{K}NN$  system can have a large width. Thus, this may provide difficulties for direct experimental observation of kaonic bound states in nuclei [16]. Many experimental efforts have been also performed to explore the pole structure of the  $K^-pp$  system. An exclusive analysis of the  $p + p \rightarrow X + K^+$ ,  $X \rightarrow p + \Lambda$  reaction at 2.85 GeV [17] indicated a large peak both in the  $\Lambda p$  invariant-mass and  $K^+$  missing-mass spectra, which had been predicted in a theoretical works [18, 19]. The observed peak corresponds to the binding energy of about 103 MeV and the width is given as  $\Gamma = 118$  MeV. The  $K^-pp$  quasi-bound state can be produced in kaon-induced reactions on light nuclei such as  ${}^3\text{He}$  and deuteron, and the signal of the resonance may be observed in the mass spectra of the final particles. The investigation for the  $K^-pp$  quasi-bound state have been further explored through  $\pi^+$  incident reaction  $d(\pi^+, K^+)K^-pp$  by E27 experiment at J-PARC [20]. The  $d(\pi^+, K^+)$  experiment also revealed a distinct peak in the  $K^+$  missing-mass spectrum, nearly at the same mass and width as the DISTO peak X. The investigation for the  $K^-pp$  quasi-bound state could be reached through the  $K^- + {}^3\text{He}$  reaction (see Fig. 1). This reaction was performed as an E15 experiment at J-PARC [21]. The E15 group suggests a broad  $K^-pp$  quasi-bound state structure at 15 MeV just below  $\bar{K}NN$  threshold [21].

The kaon-induced reactions have been studied by Koike-Harada [22] and Yamagata *et al.* [23] using the optical potential method. In Ref. [24] the  $(Y_K)_{I=0} + N \rightarrow \pi\Sigma N$  has been studied by using Faddeev approach. In this calculation they employed chiral based potentials for the  $s$ -wave  $\bar{K}N$  interaction. Within their model, they have found a clear signal corresponding to the strange-dibaryon resonances in the Faddeev scattering amplitudes and the  $(Y_K)_{I=0} + N \rightarrow \pi\Sigma N$  transition probabilities. The  $K^- + {}^3\text{He} \rightarrow \Lambda pn$  reaction was also studied by Sekihara *et*

al., [25–27] to investigate the origin of observed peak close to the  $K^-pp$  threshold in first run of E15 experiment at J-PARC [21]. Two scenarios were considered to produce the peak. In the first scenario, the  $\Lambda(1405)$  resonance can be generated but it does not correlate with  $p$ , and the uncorrelated  $\Lambda(1405)p$  system subsequently decays into  $\Lambda p$  and in the other one, the  $\bar{K}NN$  quasi-bound state should be generated and decays into  $\Lambda p$ . From the calculation of the  $\Lambda p$  invariant mass spectrum, the experimental signal was reproduced in the second scenario and they definitely discarded the scenario that the  $\Lambda(1405)$  does not correlate with  $p$ .

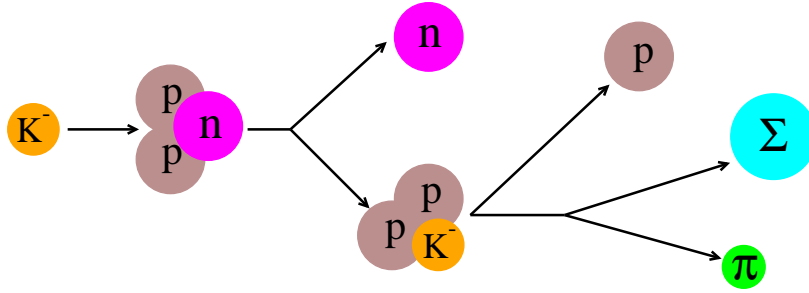


FIG. 1. Diagram for the  ${}^3\text{He}(K^-, N)K^-pp$  reactions.

This study is devoted to study the pole structure of the  $K^-pp$  three-body system. We study how well the signal  $K^-pp$  quasi-bound state can be observed in the  $\pi\Sigma N$  mass spectra resulting from reaction under consideration. We performed few-body calculations for the  $\bar{K}NN - \pi\Sigma N$  system by using coupled-channels Faddeev AGS equations. The transition probabilities for the  $(Y_K)_{I=0} + N \rightarrow \pi\Sigma N$  reaction are calculated. With this method, we investigated the behavior of the transition probability for  $(Y_K)_{I=0} + N \rightarrow \pi\Sigma N$  reaction. Several chiral based and phenomenological  $\bar{K}N - \pi\Sigma$  potentials are used [24, 28, 29] to investigate the sensitivity of the the three-body observables on two-body inputs.

The paper is organized as follows: in Sect. II, we will explain the formalism used for the coupled channel three-body  $\bar{K}NN - \pi\Sigma N$  system and give a brief description of the transition probability formula for break-up reactions. Sect. III is devoted to the two-body inputs of the calculations. The computed transition probabilities are presented in Sect. IV and in Section V, we give conclusions.

## II. THREE PARTICLE SYSTEM $\bar{K}NN - \pi\Sigma N$

The calculation of the  $\bar{K}NN - \pi\Sigma N$  three body system is based on the Faddeev treatment [30]. Separable potentials were used for describing the two-body interactions

$$V_{i,I_i}^{\alpha\beta}(k_i^\alpha, k_i^\beta; z) = g_{i,I_i}^\alpha(k_i^\alpha) \lambda_{i,I_i}^{\alpha\beta} g_{i,I_i}^\beta(k_i^\beta), \quad (1)$$

where  $g_{i,I_i}^\alpha(k_i^\alpha)$  is the form factor of the interacting two-body subsystem ( $jk$ ), with relative momentum  $k_i^\alpha$  and isospin  $I_i$ . Here,  $\lambda_{i,I_i}^{\alpha\beta}$  is the strength parameter of the interaction. To take the  $\bar{K}N - \pi\Sigma$  coupling directly into account, the potentials are further labeled with the  $\alpha$  values. The two-body  $T$ -matrices in separable form can be given by

$$T_{i,I_i}^{\alpha\beta}(k_i^\alpha, k_i^\beta; z) = g_{i,I_i}^\alpha(k_i^\alpha) \tau_{i,I_i}^{\alpha\beta}(z - E_i^\alpha(p_i^\alpha)) g_{i,I_i}^\beta(k_i^\beta), \quad (2)$$

where  $z$  and  $E_i^\alpha(p_i^\alpha)$  are the total energy of the system and the energy of the spectator particle in  $\alpha$  channel, respectively.

$$E_i^\alpha(p_i^\alpha) = \frac{(p_i^\alpha)^2}{2\nu_i^\alpha}, \quad (3)$$

the quantity  $\nu_i^\alpha = m_i^\alpha(m_j^\alpha + m_k^\alpha)/(m_i^\alpha + m_j^\alpha + m_k^\alpha)$ , is the reduced mass, when particle  $i$  in channel  $\alpha$  is spectator. The operator  $\tau_{i,I_i}^{\alpha\beta}(z - E_i^\alpha(p_i^\alpha))$  is also the usual two-body propagator. Using separable potential for two-body interactions, the three-body Faddeev equations [6] in the AGS take the form

$$\begin{aligned} \mathcal{K}_{ij,I_i I_j}^{\alpha\beta}(\vec{p}_i^\alpha, \vec{p}_j^\beta; z) &= \delta_{\alpha\beta} \mathcal{M}_{ij,I_i I_j}^{\alpha\beta}(\vec{p}_i^\alpha, \vec{p}_j^\beta; z) \\ &+ \sum_{k,I_k,\gamma} \int d\vec{p}_k^\alpha \mathcal{M}_{ik,I_i I_k}^\alpha(\vec{p}_i^\alpha, \vec{p}_k^\alpha; z) \tau_{k,I_k}^{\alpha\gamma}(z - E_k^\alpha(\vec{p}_k^\alpha)) \\ &\times \mathcal{K}_{kj,I_k I_j}^{\gamma\beta}(\vec{p}_k^\gamma, \vec{p}_j^\beta; z). \end{aligned} \quad (4)$$

After partial wave decomposition and where we assumed that only s-wave contribution will be significant in our calculations, we get the following equations

$$\begin{aligned} \mathcal{K}_{ij,I_i I_j}^{\alpha\beta}(p_i^\alpha, p_j^\beta; z) &= \delta_{\alpha\beta} \mathcal{M}_{ij,I_i I_j}^{\alpha\beta}(p_i^\alpha, p_j^\beta; z) \\ &+ \sum_{k,I_k,\gamma} \int d^3 p_k^\alpha \mathcal{M}_{ik,I_i I_k}^\alpha(p_i^\alpha, p_k^\alpha; z) \tau_{k,I_k}^{\alpha\gamma}(z - E_k^\alpha(p_k^\alpha)) \\ &\times \mathcal{K}_{kj,I_k I_j}^{\gamma\beta}(p_k^\gamma, p_j^\beta; z). \end{aligned} \quad (5)$$

Here, the operators  $\mathcal{K}_{ij,I_i I_j}^{\alpha\beta}$  are the transition amplitudes between Faddeev channels and particle channels [6]. The operators  $\mathcal{M}_{ij,I_i I_j}^{\alpha\beta}$  are the corresponding Born terms. The inputs for the AGS system of equations (5) are two-body  $T$ -matrices, embedded in the three-body Hilbert space. Faddeev partition indices  $i, j, k = 1, 2, 3$  are used to define the interacting pair and also the spectator particle. The Faddeev equations are modified [6, 7] to take the  $\bar{K}N - \pi\Sigma$  coupling directly into account. Thus, in addition to the Faddeev indices the particle indices ( $\alpha, \beta, \gamma = 1, 2, 3$ ) are also added for each state ( $i$ ) [31].

$$\alpha = \{1, 2, 3\} = \{\bar{K}NN, \pi\Sigma N_2, \pi N_1\Sigma\}.$$

Since the total isospin of the system is  $I = 1/2$ , therefore, depending on the spin of the two baryons, we should treat  $K^-pp$  or  $K^-d$  system. The total spin of the system remains unchanged. Therefore, the baryon spins do not enter explicitly and the operators will be labeled by isospin indices. In the  $K^-pp$  system the spin component is antisymmetric, so all operators in isospin base should be symmetric.

In present Calculations, we used the quasi-particle approach to solve the Faddeev equations for bound state problem. The most important part of the quasi-particle method is the separable expansion of the scattering amplitudes in the two- and three-body systems [32–34]. To find the  $K^-pp$  pole position, the separable representation must be defined for the three-body amplitudes and driving terms. For this purpose, we used the Hilbert-Schmidt expansion method [33, 35].

$$\begin{aligned} \mathcal{M}_{ij,I_i I_j}^{\alpha}(p_i^{\alpha}, p_j^{\alpha}; z) &= - \sum_{n=1} \lambda_n(z) u_{n;i,I_i}^{\alpha}(p_i^{\alpha}; z) \\ &\times u_{n;j,I_j}^{\alpha}(p_j^{\alpha}; z), \end{aligned} \quad (6)$$

the form factors  $u_{n;i,I_i}^{\alpha}(p_i^{\alpha}, z)$  are taken as the eigenfunctions of the kernel of the equation (5). The separable form of the Faddeev transition amplitudes is given by

$$\mathcal{K}_{ij,I_i I_j}^{\alpha\beta}(p_i^{\alpha}, p_j^{\beta}; z) = \sum_n u_{n;i,I_i}^{\alpha}(p_i^{\alpha}; z) \zeta_n(z) u_{n;j,I_j}^{\beta}(p_j^{\beta}; z), \quad (7)$$

where the functions  $\zeta_n(z)$  obey the equation

$$\zeta_n(z) = \lambda_n(z)/(\lambda_n(z) - 1). \quad (8)$$

Applying Hilbert-Schmidt expansion method [35] to the Faddeev equations of  $\bar{K}NN - \pi\Sigma N$ ,

the following homogeneous integral equations for  $u_{n;i,I_i}^\alpha(p_i^\alpha; z)$  are obtained

$$u_{n;i,I_i}^\alpha(p_i^\alpha; z) = \frac{1}{\lambda_n} \sum_{\gamma,k=1}^3 \sum_{I_k} \int d^3 p_k^\alpha \mathcal{M}_{ik,I_i I_k}^\alpha(p_i^\alpha, p_k^\alpha; z) \times \tau_{k,I_k}^{\alpha\gamma}(z - E_k^\alpha(p_k^\alpha)) u_{n;k,I_k}^\gamma(p_k^\gamma; z). \quad (9)$$

To solve the homogeneous system, we should search for a complex energy at which one of the eigenvalues ( $\lambda_n(z)$ ) of the kernel matrix becomes equal to one. We must work on the physical and unphysical energy sheet of the  $\bar{K}NN$  and  $\pi\Sigma N$  channels, respectively.

Another purpose of this work is to study the possible signature of the  $K^-pp$  quasi-bound state in the  $\pi\Sigma N$  mass spectra from the reaction  $(Y_K)_{I=0} + N \rightarrow \pi\Sigma N$ . The break-up amplitude for this reaction in terms of the Faddeev transition amplitudes can be given by [36].

$$\begin{aligned} & T_{\pi\Sigma N \leftarrow (Y_K)_{I=0} + N}(\vec{k}_N, \vec{p}_N, p'_N; z) \\ &= \sum_I g_{\pi\Sigma, I}(\vec{k}_N) \tau_{(\pi\Sigma)_{IN}, (\bar{K}N)_{IN}}(z - E_N(\vec{p}_N)) \\ &\quad \times \mathcal{K}_{(\bar{K}N)_{IN}, (\bar{K}N)_{I=0}N}(p_N, p'_N; z) \\ &+ \sum_I g_{\pi\Sigma, I}(\vec{k}_N) \tau_{(\pi\Sigma)_{IN}, (\pi\Sigma)_{IN}}(z - E_N(\vec{p}_N)) \\ &\quad \times \mathcal{K}_{(\pi\Sigma)_{IN}, (\bar{K}N)_{I=0}N}(p_N, p'_N; z) \\ &+ \sum_I \sum_{I'} \langle [\pi \otimes \Sigma]_{I'} \otimes N \mid \pi \otimes [\Sigma \otimes N]_I \rangle g_{\Sigma N, I}(\vec{k}_\pi) \\ &\quad \times \tau_{\pi(\Sigma N)_I, \pi(\Sigma N)_I}(z - E_\pi(\vec{p}_\pi)) \\ &\quad \times \mathcal{K}_{\pi(\Sigma N)_I, (\bar{K}N)_{I=0}N}(p_\pi, p'_N; z), \end{aligned} \quad (10)$$

where  $z$  is the three-body energy. To find the two-body energy, we should reduce it by spectator particle energy  $E_i(\vec{p}_i)$ . Here,  $\vec{k}_i$  is the relative momentum between the interacting pair ( $jk$ ). The quantities  $\mathcal{K}_{i,j}$  are Faddeev amplitudes, which are derived from Faddeev equation (5). Since the  $\pi N$  interaction is neglected, in this equation the Faddeev transition amplitudes corresponding to  $\pi N$  system are missing. Using Eq.(10), we define the transition probability of  $(Y_K)_{I=0} + N \rightarrow \pi\Sigma N$  as follows,

$$w(p'_N, z) = \int d^3 p_N \int d^3 k_N \delta(z - Q(p_N, k_N)) \times |T_{\pi\Sigma N \leftarrow (Y_K)_{I=0} + N}(\vec{k}_N, \vec{p}_N, p'_N; z)|^2. \quad (11)$$

where  $Q(p_N, k_N)$  is given by

$$Q(p_N, k_N) = \frac{p_N^2(m_N + m_\pi + m_\Sigma)}{2m_N(m_\pi + m_\Sigma)} - \frac{k_N^2(m_\pi + m_\Sigma)}{2m_\pi m_\Sigma} \quad (12)$$

### III. TWO-BODY INPUT

In this section, we give a brief survey on two-body interactions, which are the central inputs for the present few-body calculations. The  $\bar{K}N - \pi\Sigma$  interaction is dominated by the  $s$ -wave  $\Lambda(1405)$  resonance. Therefore, the orbital angular momentum for  $\bar{K}N$  interaction is taken to be zero. The  $NN$  and  $\Sigma N$  interactions were also taken in  $l = 0$  state. Since, the interaction in  $\pi N$  subsystem is dominated by the  $p$ -wave component. Thus, in our few-body calculations the  $\pi N$  interaction is neglected. All separable potentials in momentum representation have the form of Eq. (1).

#### A. $\bar{K}N - \pi\Sigma$ coupled-channel system

During the past two decades, different phenomenological [1, 28, 37] and chiral based [38–44] potentials are constructed to describe the  $\bar{K}N$  interaction. The phenomenological models of interaction consider the  $\Lambda(1405)$  resonance as a quasi-bound in  $\bar{K}N$  system embedded in the  $\pi\Sigma$  continuum. The chiral SU(3) dynamics has also turned out to be a successful approach to describe the  $\bar{K}N$  interaction and the  $\Lambda(1405)$  resonance [38–44]. At and above  $\bar{K}N$  threshold, the phenomenological and the chiral SU(3)  $\bar{K}N$  models of interaction produce comparable results, while for subthreshold energies their results are different. The phenomenological  $\bar{K}N$  interactions are constructed to reproduce a single pole nature for the  $\Lambda(1405)$  resonance as a quasi-bound state of the  $\bar{K}N$  system around 1405 MeV. The  $\bar{K}N - \pi\Sigma$  coupled-channels amplitude resulting from chiral SU(3) based potentials has two poles, one of them is located around 1420 MeV [39]. while the other pole with large width is located above the  $\pi\Sigma$  threshold. Therefore, the chiral based potentials produce a binding energy of about 15 MeV for  $\bar{K}N$  system, which is about half the binding produced with the purely phenomenological  $\bar{K}N$  models of interaction.

We used different models to describe the  $s$ -wave  $\bar{K}N - \pi\Sigma$  interaction, which is the most important interaction in the present three-body calculations with  $\bar{K}NN$  and  $\pi\Sigma N$  coupled-channels. We considered four types of phenomenological potentials. They reproduce the one- and two-pole structure for  $\Lambda(1405)$  resonance and their parameters are given in Refs. [28, 29]. The parameters are adjusted to reproduce all existing data on low-energy  $\bar{K}N$  interaction. The  $\bar{K}N - \pi\Sigma$  potentials in Ref. [29] are adjusted to reproduce the experimental results of the SIDDHARTA experiment [45]. Depending on a pole structure of the  $\Lambda(1405)$ , we refer these potentials as “SIDD, one-pole” and “SIDD, two-pole” potential. The parameters of the potentials in Ref. [28] are adjusted to

reproduce the experimental results of the KEK experiment [46, 47]. Depending on a pole structure of the  $\Lambda(1405)$ , we refer these potentials as “KEK, one-pole” and “KEK, two-pole” potential.

Plus the phenomenological potentials, we also used two chiral based  $\bar{K}N - \pi\Sigma$  potentials, which are given in Ref. [24]. These chiral based potentials reproduce the elastic and inelastic cross sections for the  $K^-p$  reaction as well as the  $\pi\Sigma$  mass spectra.

## B. $NN$ interaction

In order to investigate the dependence of the  $\pi\Sigma N$  invariant mass on nucleon-nucleon interaction models, we used two different potentials for  $NN$  interaction. The first one is a two-term separable potential [48]

$$V_{NN}^I = \sum_{m=1}^2 g_{NN}^{I,m}(k) \lambda_{NN}^{I,m} g_{NN}^{I,m}(k'), \quad (13)$$

where  $\lambda_{NN}^{I,1}$  is negative to take into account the short range repulsion part of the interaction. The parameters of this potential are given in Ref. [48].

We also used one-term PEST potential from Ref. [49]. The strength parameter of the PEST potential is equal to one and the form-factor is defined by

$$g_{NN}^I(k) = \frac{1}{2\sqrt{\pi}} \sum_{i=1}^6 \frac{c_{i,I}^{NN}}{(\beta_{i,I}^{NN})^2 + k^2}, \quad (14)$$

where the parameters of the potential are given in Ref. [49]. The PEST potential is not repulsive at short distances, but at low energies its phase shifts are close to the rank-two potential.

For the  $s$ -wave  $\Sigma N$  interaction, we follow the form given in Ref. [50],

$$V_{\alpha\beta}^I(k^\alpha, k^\beta) = -\frac{C_{\alpha\beta}^I}{2\pi^2} (\Lambda_\alpha \Lambda_\beta)^{3/2} (\mu_\alpha \mu_\beta)^{-1/2} g_\alpha^I(k^\alpha) g_\beta^I(k^\beta). \quad (15)$$

where the form factor defined by  $g_\alpha^I(k^\alpha) = 1/((k^\alpha)^2 + \Lambda_\alpha^2)$ . The coupling constants,  $C_{\alpha\beta}^I$ , and the range parameters  $\Lambda_\alpha$  are given in Ref. [50].

## IV. RESULTS AND DISCUSSION

Solutions of the Faddeev equations corresponding to bound states and resonance poles in the  $(I, J^\pi) = (\frac{1}{2}, 0^-)$  channel of the  $\bar{K}NN - \pi\Sigma N$  three-body system were found by applying search procedures described in Sec. II. In Table I and II, the results of the present work for three-body



$\bar{K}NN - \pi\Sigma N$  quasi-bound state are presented. The sensitivity of the  $\bar{K}NN$  pole position to the  $\bar{K}N - \pi\Sigma$  interaction is investigated by using different potential models. In Table I the pole position of the quasi-bound states in the  $\bar{K}NN$  systems is calculated for phenomenological models of the  $\bar{K}N - \pi\Sigma$  interaction and in Table II, we calculated the pole energies for energy-dependent and energy-independent chiral potentials.

TABLE I. The sensitivity of the pole position(s) (in MeV),  $z_X^{pole}$ , of the  $\bar{K}N$  and  $\bar{K}NN$  systems to the different phenomenological models of the  $\bar{K}N - \pi\Sigma$  interaction is investigated.  $V_{\bar{K}N-\pi\Sigma}^{One-pole}$  and  $V_{\bar{K}N-\pi\Sigma}^{Two-pole}$  standing for a one- and a two-pole structure of the  $\Lambda(1405)$  resonance, respectively.

	$V_{\bar{K}N-\pi\Sigma}^{One-pole}$	$V_{\bar{K}N-\pi\Sigma}^{Two-pole}$
SIDD pot. [28]:		
$z_{\bar{K}N}^{pole}$	1428.1 - i46.6	1418.1 - i56.9 1382.0 - i104.2
$z_{\bar{K}NN}^{pole}$	2320.7 - i31.5	2325.0 - i24.1
KEK pot. [29]:		
$z_{\bar{K}N}^{pole}$	1411.3 - i35.8	1410.8 - i35.9 1380.8 - i104.8
$z_{\bar{K}NN}^{pole}$	2329.0 - i26.0	2327.6 - i19.5

TABLE II. The pole position(s) (in MeV),  $z_X^{pole}$ , of the quasi-bound states in the  $\bar{K}N$  and  $\bar{K}NN$  systems is calculated for energy-dependent and energy-independent chiral potentials.

	$V_{\bar{K}N-\pi\Sigma}^{E-indept.}$	$V_{\bar{K}N-\pi\Sigma}^{E-dept.}$
$z_{\bar{K}N}^{pole}$	1407.2 - i18.5	1420.6 - i20.3 1343.0 - i72.5
$z_{\bar{K}NN}^{pole}$	2313.4 - i21.9	2346.5 - i22.0

The position of a quasi-bound state in the three-body problem is usually defined by solving the homogeneous integral equations (9) which comes from the separable expansion of the Faddeev amplitudes. To find the resonance energy of the system using these equations, one should search for a complex energy at which one of the eigenvalues of the kernel matrix becomes equal to one. Therefore, as one can see from Eqs. 7 and 8, the Faddeev amplitudes will have a pole at this energy.

To examine the efficiency of the separable expansion method, we used another way to find the  $K^-pp$  pole position(s) without using the integration in the complex momentum plane. The signal of the  $K^-pp$  bound state would be seen in the Faddeev transition amplitudes. In the present work, we studied how the signature of the  $K^-pp$  quasi-bound state shows up in the three-body scattering amplitudes by using coupled-channel Faddeev AGS equations. To achieve this goal, we must solve the inhomogeneous integral equations for the amplitudes defined in Eq. (5).

Fig. 2 shows the calculated three-body scattering amplitude  $|\mathcal{K}_{(\bar{K}N)_{I=0}+N \rightarrow (\bar{K}N)_{I=0}+N}(p_N, p'_N; z)|$  whose initial and final states are  $(\bar{K}N)_{I=0} + N$ . The off-shell momenta  $p$  and  $p'$  are equal, 150 MeV/c and the real and imaginary part of the three-body energy,  $z$ , change from -100 MeV to 0 MeV. We used one-pole (left) and two-pole (right) version of the KEK potential for describing the  $\bar{K}N - \pi\Sigma$  interaction. Since the input energy of the AGS equations is complex the moving singularities which are caused by the open channel  $\pi\Sigma N$ , will not appear in the three-body amplitudes. The calculated resonance energies of the  $\bar{K}NN$  system by this method, have presented in Table III. Comparing these results with those in Table I, one can see that both results are in good agreement with each other.

When at least one of the intermediate particles is unstable, plus the signal of the resonance states, one can see a branch point in the complex plane. In Fig. 2, plus the signature of  $K^-pp$  pole position, we can see the branch points i.e., a threshold opening associated with the  $\Lambda(1405)$  pole, situated at  $z = M_N + M_{\Lambda(1405)}$ , sum of nucleon mass and  $\Lambda(1405)$  pole position. In the second row of Fig. 2, we have shown the branch points for  $\Lambda(1405)N$  intermediate state. The branch point is clearly visible, together with the cut that in this picture is chosen in the positive  $\text{Re } z$  direction. In the second row, to make the branch points more visible the imaginary part of the three-body energy,  $z$ , was chosen to be between -50 MeV and -12 MeV and the real part change from 2347 MeV to 2375 MeV. We used one-pole (left) and two-pole (right) version of the KEK potential to extract the branch points.

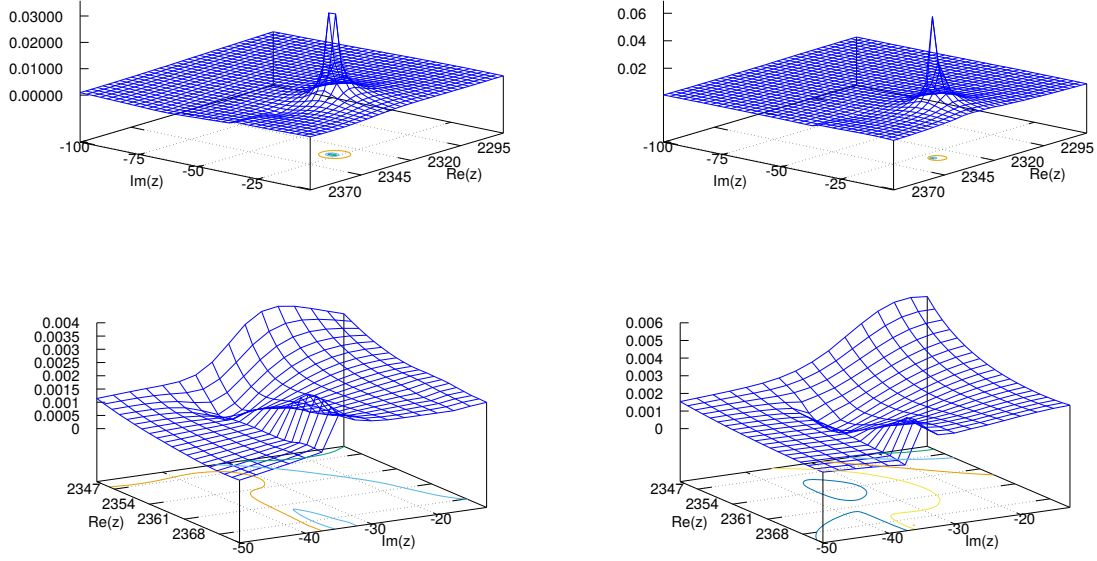


FIG. 2. (Color online) The Faddeev amplitude for  $(\bar{K}N)_{I=0} + N \rightarrow (\bar{K}N)_{I=0} + N$  reaction. The transition amplitudes calculated using one-pole (left) and two-pole (right) models of KEK potential. In second row, the imaginary part of  $z$ , was chosen to be between  $-50$  MeV and  $-12$  MeV and the real part change from  $2347$  MeV to  $2375$  MeV to make the branch points more visible. The three-body calculations performed by using the PEST potential model for  $NN$  interaction.

TABLE III. The pole position (in MeV) of the Faddeev amplitude for  $(\bar{K}N)_{I=0} + N \rightarrow (\bar{K}N)_{I=0} + N$  reaction. The pole positions are calculated for one- and two-pole models of KEK potential.

	$V_{\bar{K}N-\pi\Sigma}^{KEK,One-pole}$	$V_{\bar{K}N-\pi\Sigma}^{KEK,Two-pole}$
$z_{\bar{K}NN}^{pole}$	$2331.0 - i27.2$	$2328.5 - i19.8$

We investigated the dependence of the two- and three-body pole energy trajectories on the magnitude  $\lambda_{\bar{K}N-\bar{K}N}^{I=0}$ , when the  $\bar{K}N$  strength parameter is increased from its physical value. Let  $\kappa$  stand for an enhancement factor of strength of the  $I = 0$   $\bar{K}N$  interaction:

$$\bar{\lambda}_{\bar{K}N-\bar{K}N}^{I=0} = \kappa \lambda_{\bar{K}N-\bar{K}N}^{I=0}. \quad (16)$$

We calculated the pole trajectory for one- and two-pole version of the KEK potential. The

behavior of the two-body  $K^-p$  and three-body  $K^-pp$  pole energy trajectories are quite different at  $\pi\Sigma$  threshold. The pole energies obtained for three-body system are shown in Fig. 3 (B). The blue dashed and black solid curves in Fig. 3 (A) correspond to the two-body results. The numbers attached to the circles and squares give the corresponding values of the enhancement factor  $\kappa$ . As  $\kappa$  increases, the binding energy of the system increases for both the two- and three-body systems. In the two-body calculations of two-pole potential, the imaginary part of the resonance energy becomes smaller as the binding energy increases and for  $\kappa \sim 1.33$  (at  $\pi\Sigma$  threshold) the resonance almost becomes a bound state in  $\pi\Sigma$  channel. In contrary, in the three-body system the resonance energy will have a non zero imaginary part at the  $\pi\Sigma$  threshold as  $\kappa$  grows, since the  $\pi\Lambda$  channel is included effectively.

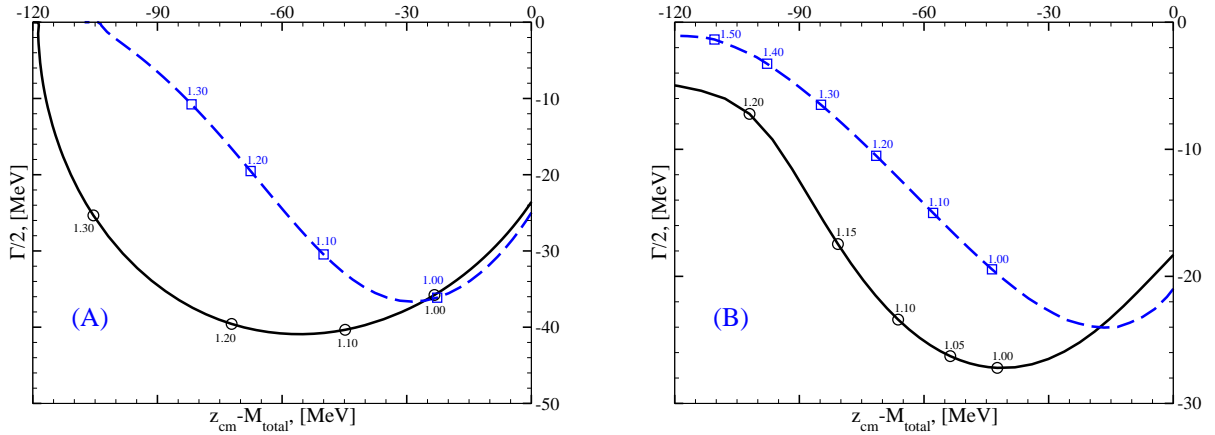


FIG. 3. (Color online) Resonance energy of  $\bar{K}N$  (A) and  $\bar{K}NN - \pi\Sigma N$  (B) systems. The numbers attached to the squares and circles give the corresponding values of the enhancement factor  $\kappa$  in Eq. (16). The resonance energies calculated using KEK potentials for  $\bar{K}N - \pi\Sigma$  interaction given in Ref. [28]. These potential models can reproduce the one- and two-pole structure of  $\Lambda(1405)$  resonance. The solid lines show the resonance energies with one-pole model, and the dashed lines show the resonance energies with the two-pole model of the KEK potential. Here,  $z_{cm}$  is the energy of the system in center of mass frame and  $M_{total}$  is the mass of the two- and three-body system.

### A. Calculation of the transition probability

The calculated resonance energies that have presented in Table I and II, give only pole positions of the  $K^-pp$  system. However, we know that these results are not a quantity that can be directly measured in any experiments. To examine the existence of the quasi-bound state in  $K^-pp$  system

by experiments, one has to calculate the cross sections of  $K^-pp$  production reactions. We can use the calculated results in Table I and II and also in Fig. 3 as guideline to study these reactions. As it was said in Sect. I, the  $K^-pp$  quasi-bound state can be produced through kaon-induced reactions on light nuclei such as  $^3\text{He}$  and deuteron. The trace of the resonances would be seen in the mass spectra of the final particles. In the present calculations, we studied how good the signature of the  $K^-pp$  system shows up in the observables of the three-body reactions by using coupled-channel Faddeev equations in the AGS form. To achieve this goal, we must solve the coupled integral equations for the amplitudes defined in Eq. (5), and then construct the breakup amplitudes  $T_{\pi\Sigma N \leftarrow (Y_K)_{I=0} + N}$  defined in Eq. (10). Since the kernel of AGS equations has the standard moving singularities that are caused by the opened channel  $\pi\Sigma N$  and are encountered in any three-body breakup problem, we have followed the same procedure implemented in Refs. [51, 52]. Using the so called “point-method”, we computed the cross section of  $(Y_K)_{I=0} + N \rightarrow \pi\Sigma N$  reaction and studied the behavior of  $\pi\Sigma N$  mass spectra. The transition probabilities for phenomenological potentials are depicted in Figs. 4 and 5. In Fig. 6 the three-body calculations are performed by chiral based potentials for  $\bar{K}N$  interaction and PEST potential for  $NN$  interaction.

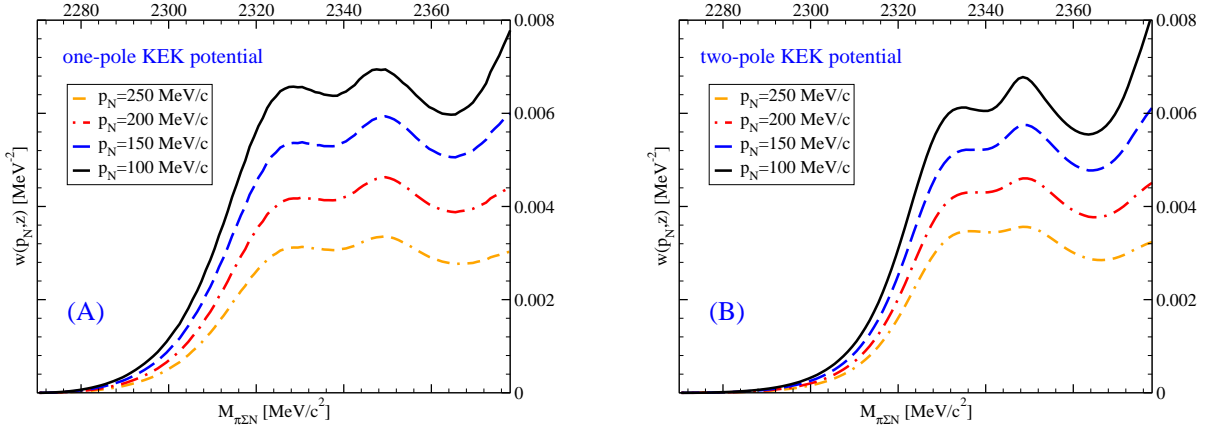


FIG. 4. (Color online) The  $\pi\Sigma N$  mass spectra for  $(Y_K)_{I=0} + N \rightarrow \pi\Sigma N$  reaction. The  $M_{\pi\Sigma N}$  spectra calculated using KEK potentials for  $\bar{K}N - \pi\Sigma$  interaction given in Ref. [28]. The calculations are performed by using the PEST potential for  $NN$  interaction. To investigate the energy dependence of the transition probability, we calculated  $w(p_N, z)$  for  $p_N = 100 - 250$  MeV/c.

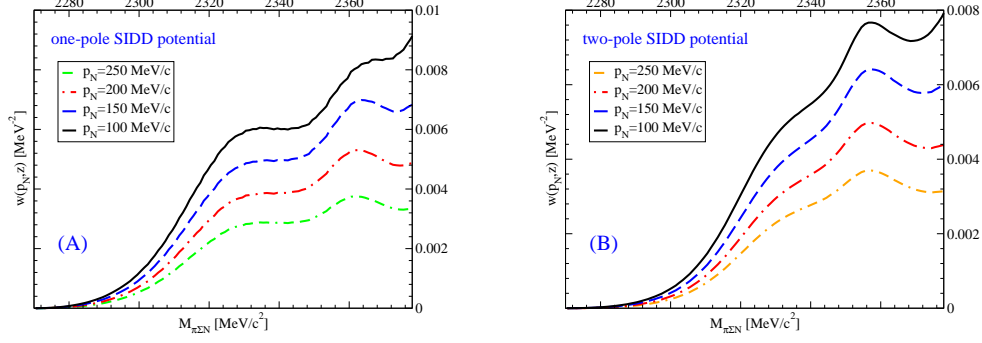


FIG. 5. (Color online) Same as Fig.4 but using SIDDHARTA potentials [29] for  $\bar{K}N - \pi\Sigma$  interaction which reproduce the one- and two-pole structure of  $\Lambda(1405)$  resonance.

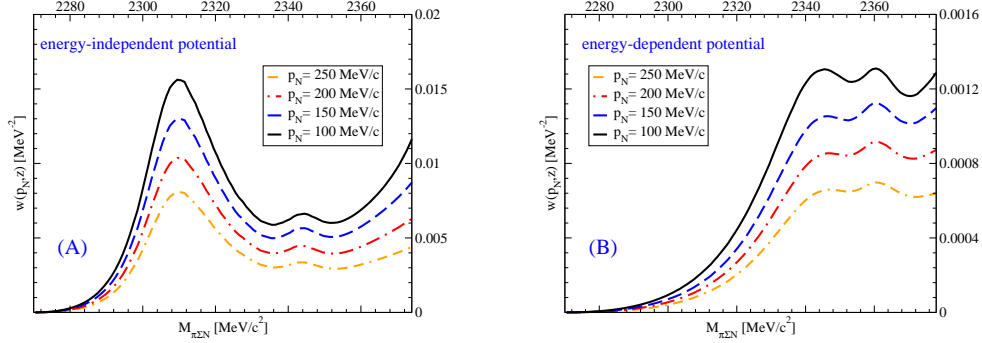


FIG. 6. (Color online) Same as Fig.4 but for the energy-dependent (B) and energy-independent (A) potentials given in Ref. [24].

TABLE IV. The dependence of the  $\bar{K}N$  (first pole) and  $\bar{K}NN$  quasi-bound state positions (in MeV) on the  $\lambda_{\bar{K}N-\bar{K}N}$  strength parameter in the  $I = 0$  state. We calculated the pole positions for three values of  $\kappa$  parameter.

	$\kappa = 1.00$	$\kappa = 1.05$	$\kappa = 1.10$
$z_{\bar{K}N}^{pole}$	1420.6 - $i$ 20.25	1414.4 - $i$ 21.8	1407.7 - $i$ 24.0
$z_{\bar{K}N(+N)}^{pole}$	2359.5 - $i$ 20.25	2353.3 - $i$ 21.8	2346.6 - $i$ 24.0
$z_{KNN}^{pole}$	2346.5 - $i$ 22.0	2339.0 - $i$ 22.1	2331.6 - $i$ 21.5

In Fig. 4, we calculated the  $\pi\Sigma N$  mass spectra using one-pole (A) and two-pole (B) version of KEK potentials for  $\bar{K}N - \pi\Sigma$  interaction given in Ref. [28]. To investigate the energy dependence

of the transition probability, we calculated  $w(p_N, z)$  for  $p_N = 100 - 250$  MeV/c. We investigated the dependence of  $\pi\Sigma N$  mass spectra on two-body  $\bar{K}N - \pi\Sigma$  interactions, necessary for the description of the  $\bar{K}NN - \pi\Sigma N$  system. Therefore, in Fig. 5, we calculated the  $\pi\Sigma N$  mass spectra using the one- and two-pole version of the SIDDHARTA potential for  $\bar{K}N - \pi\Sigma$  interaction given in Ref. [28]. The results suggest that a distinct peak of bound kaonic states should be observed, regardless of the momentum value and the class of the  $\bar{K}N - \pi\Sigma$  interaction. In the calculated mass spectra for the two-pole model of the KEK and SIDDHARTA potentials, the second pole of  $\Lambda(1405)$  resonance with its large width, does not affect the  $\pi\Sigma N$  invariant mass. As one can see from Figs. 4 and 5, all potential models will produce the mass spectra with the similar behavior and two distinct bump structures can be seen in the  $\pi\Sigma N$  invariant mass.

The results of the full coupled-channel calculations of the  $(Y_K)_{I=0} + N \rightarrow \pi\Sigma N$  scattering using two versions of the energy-dependent and energy-independent  $\bar{K}N - \pi\Sigma$  potentials derived based on chiral SU(3) dynamic and non relativistic kinematics are shown in Fig. 6. It is seen, that the three-body results corresponding to each version of  $\bar{K}N$  interaction differ sufficiently. Therefore, in principle, it would be possible to favor one version of the  $\bar{K}N - \pi\Sigma$  potential by comparing with experimental results. Within this model, we have found two bump structures appearing in the  $(Y_K)_{I=0} + N \rightarrow \pi\Sigma N$  transition probabilities in the energy region around the  $\bar{K}NN$  pole position and  $z = M_N + M_{\Lambda(1405)}$ . As it was said before, the second bump which is situated at  $z = M_N + M_{\Lambda(1405)}$  is actually originated from a branch point in the complex plane (see Fig.2), i.e., a threshold opening associated with the  $\Lambda(1405)$  pole.

To show that, these bumps are really corresponding to the quasi-bound state in the  $\bar{K}NN$  system and  $\Lambda(1405)$  pole and are not caused by threshold effects. Let us investigate these bump structures in the  $\pi\Sigma N$  mass spectra and clarify the origin of these bumps. In Fig. IV A, we calculated the  $\pi\Sigma N$  mass spectra using one- and two-pole version of the KEK and also energy-dependent chiral potentials for  $\bar{K}N - \pi\Sigma$  interaction when the magnitude of the ( $I = 0$ )  $\bar{K}N$  strength parameter is increased from its physical value. We calculated the  $\pi\Sigma N$  mass spectra for three values of the enhancement factor  $\kappa = 1.0, 1.05$  and  $1.10$ . As it was shown in Fig. 3 and Table IV, when we increase the  $\kappa$  parameter, the binding energy of the system will increase for both the two- and three-body systems and the pole energies will go toward the  $\pi\Sigma(+N)$  and  $\pi\Sigma N$  threshold, respectively. Comparing the results of the mass spectra with those presented in Table IV and Fig. 3, one can see that the bump structures in the mass spectra and the quasi-bound states in Table IV will locate at the same energy and have the same movement. Therefore, one can say that

the first bump structure should be corresponding to a quasi-bound state in  $\bar{K}NN$  system and the second bump structure is derived from a branch point in the complex plane.

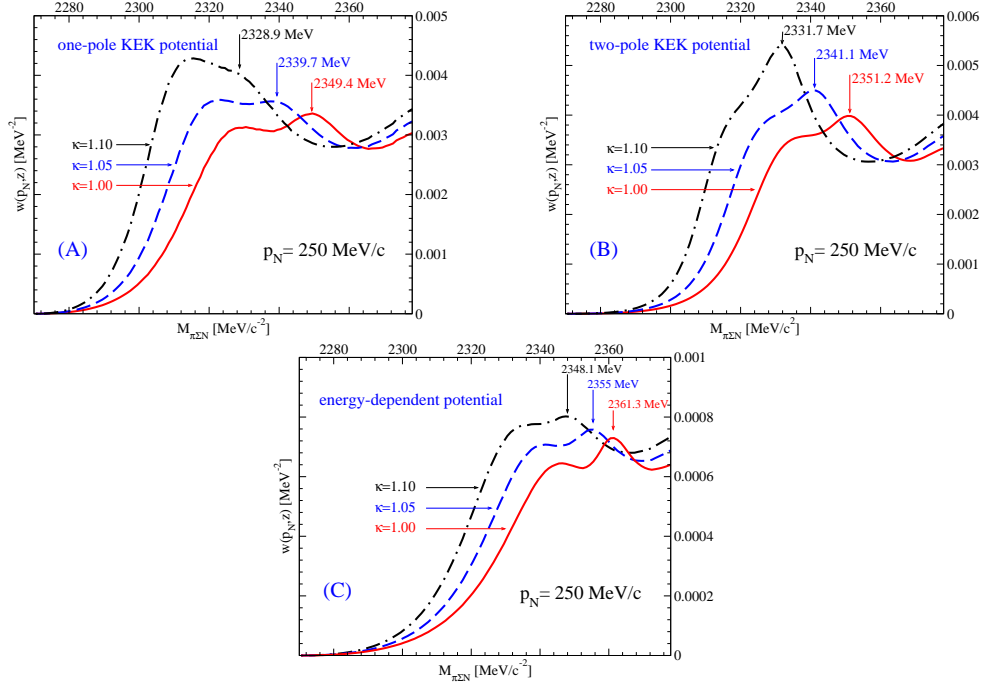


FIG. 7. (Color online) Our results for  $\pi\Sigma N$  mass spectra are presented using “KEK, one-pole”, “KEK, two-pole” and also energy-dependent potentials for  $\bar{K}N$  interaction and PEST potential for  $NN$  interaction. We calculated the  $\pi\Sigma N$  invariant mass for three different values of the  $\kappa$  coefficient. As one can see, when we increase the  $\kappa$  parameter, the movement of the bumps location are very similar to the movement of the pole positions in the  $\bar{K}N(+N)$  and  $\bar{K}NN$  systems, which are presented in Table IV and Fig. 3.

In order to compare the present results with those in Ref. [24], we calculated  $w(p_N, z)$  for  $p_N = 100$  MeV/c using the same  $\bar{K}N - \pi\Sigma$  and a two-term type potential [48] with a repulsive core and an intermediate-range attraction is used to describe the nucleon-nucleon interaction. The  $\pi\Sigma N$  invariant mass obtained with the two-terms  $V_{NN}^I$  are shown in Fig. 8. Energy-dependent set of  $\bar{K}N - \pi\Sigma$  potential was used together.

In contrast to the results of Ref. [24], our results show that, plus the bump related to the quasi-bound state in  $\bar{K}NN$  systems, a typical bump structure manifests itself in the  $\pi\Sigma N$  invariant mass at the energy related to the quasi-bound state in  $\bar{K}N(+N)$  system. However, this bump structure in the observables dose not derives from a resonance pole and the origin of this structure is the branch points. The behavior of the mass spectra is similar to the extracted results for the



phenomenological potentials. The difference between the present results and those by Ohnishi *et al.*, can be important. In our results, we have two bump structure close to each other in the mass spectra, one is related to the quasi-bound state in  $K^-pp$  system and the other corresponding to branch points which originates from intermediate  $\Lambda(1405)$ . Thus, this effect should be taken into account in theoretical interpretation of the experimental results by E15.

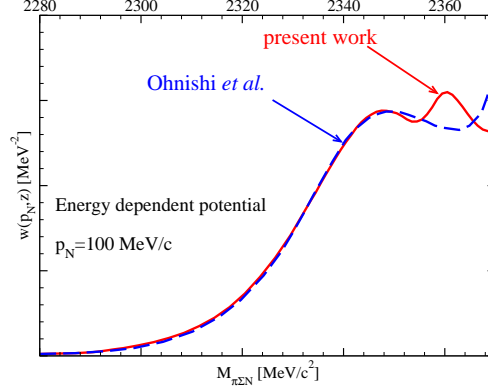


FIG. 8. (Color online) The calculated  $\pi\Sigma N$  mass spectra for energy-dependent potential is compared with other theoretical results. The  $\pi\Sigma N$  mass spectra for incident momentum  $p_N = 100$  MeV/c was calculated. Our result is shown by red solid curve and the result by Ohnishi *et al.* [24] by blue dashed curve.

## B. Averaged transition probability

In Subsection IV A, we calculated the transition probabilities for four discrete values of momentum, but, in actual situation the momentum  $p'_N$  can occupy any value over a continuous range. To include all these momenta into consideration, in this subsection, we calculated the averaged transition probability  $\bar{w}$ , which is given by

$$\begin{aligned} \bar{w}(z) = & \int d^3 p_N \int d^3 k_N \delta(z - Q(p_N, k_N)) \\ & \times \left| \int p_N'^2 dp_N' \rho(p_N') T_{\pi\Sigma N \leftarrow (Y_K)_{I=0+N}}(\vec{k}_N, \vec{p}_N, p_N'; z) \right|^2. \end{aligned} \quad (17)$$

where the function  $\rho(p_N)$  can be defined by

$$1 = \langle \psi | \psi \rangle = \int_0^\infty p_N^2 dp_N \rho(p_N). \quad (18)$$

To define the wave function of the  $K^-pp$  three-body system, we used the so called "exact optical" potential [28]. Therefore the  $\pi\Sigma N$  channel has not included directly into account and

we can drop the particle channel indices. Using Faddeev equations in 9, we can calculate three Faddeev components,  $\phi_{i,I_i}^\alpha(p_i, k_i; z)$ , which are given by

$$\begin{aligned} \phi_{i,I_i}(p_i, k_i; z) &= \frac{1}{z - k_i^2/2\mu_i - p_i^2/2\nu_i} \\ &\times g_{i,I_i}(k_i)\tau_{i,I_i}(z - E_i(p_i))u_{n,i,I_i}(p_i, z), \end{aligned} \quad (19)$$

where  $\mu_i = \frac{m_j m_k}{m_j + m_k}$  is the reduced mass of the interacting pairs  $jk$  and also  $p_i$  and  $k_i$  are the Jacobi momenta of the spectator particle and interacting particles, respectively. The  $K^-pp$  three-body wave function can be defined by

$$|\psi\rangle = \sum_{i,I_i} |\phi_{i,I_i}\rangle, \quad (20)$$

where  $\psi$  is the normalized wave function of the  $K^-pp$  system, which is defined as a sum of the above components. Figure IV B (up) shows the momentum distribution of the spectator nucleon,  $\rho_N(p)$ , in  $K^-pp$  system for various models of the  $\bar{K}N - \pi\Sigma$  potential and Figure IV B (down) shows the same distributions but multiplied by  $p_N^2$ .

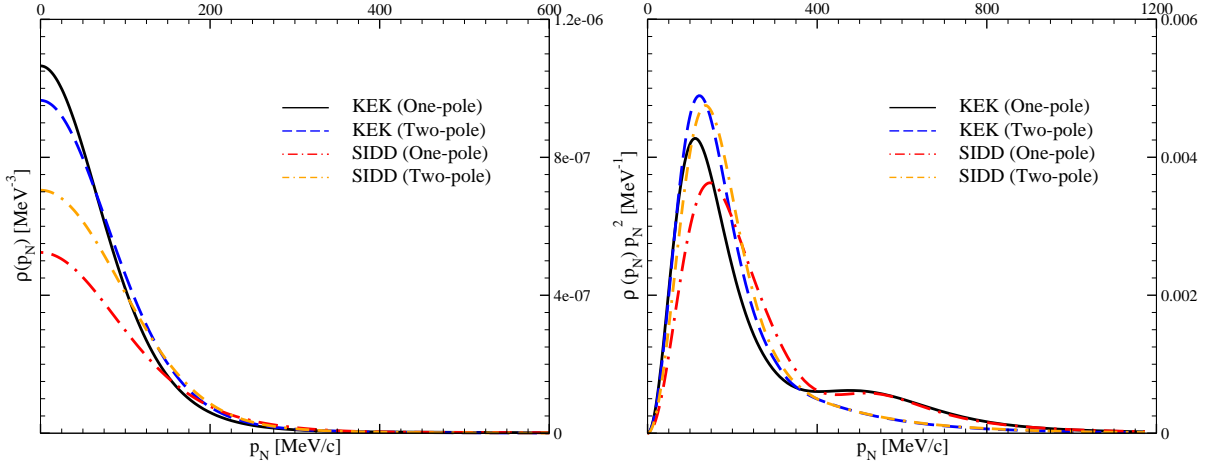


FIG. 9. (Color online) The momentum distribution of the spectator nucleon, (up)  $\rho(p_N)$  and (down)  $p_N^2\rho(p_N)$ , in  $K^-pp$  system. We used different kind of potentials to study the model dependence of the momentum distributions.

[H]

Fig. 10 shows the calculated  $\pi\Sigma N$  mass spectra using one- and two-pole version of KEK (black curves) and SIDD potential (blue curves) for  $\bar{K}N - \pi\Sigma$  interaction. As one can see, the mass spectra around the  $\bar{K}NN$  threshold are affected by the kinematical effects and the peaks corresponding

to the  $\Lambda(1405) + N$  branch point and  $K^-pp$  quasi-bound states are not as clear as in Figs. 4 and 5. According to the Figs. 4, 5 and IV B, these changes were expected, because the threshold effects are stronger for low values of the  $p'_N$  momentum and the weight of them in the momentum distribution are larger than high momentum.

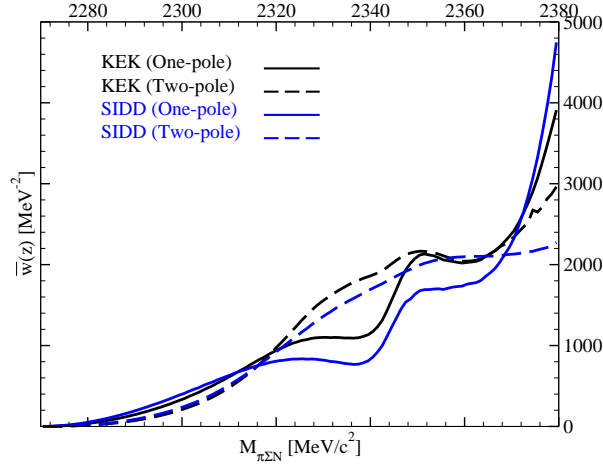


FIG. 10. (Color online) Energy dependence of the averaged transition probability,  $\bar{w}(z)$ . To study the model dependence of the results, we used KEK potential (black curves) and SIDD potentials (blue curves) in our calculations. The solid curves represent the results of the one-pole models and the dashed curves belong to the two-pole models.

In general, Faddeev equations need as input a potential that describes the interaction between two individual particles. It is also possible to introduce a term in the equation in order to take three-body forces into account. Although, we think, that while our information about the two-body  $\bar{K}N$  interaction is not completed, the inclusion of three-body forces can not be necessary. One can also investigate the dependence of the mass spectra on the two-body local potentials [44]. The three-body theory of reactions can also be formulated for local potentials on the basis of the Faddeev equations. The work in this direction is underway and will be reported elsewhere.

## V. CONCLUSION

In summary, in this work exact Faddeev-type calculations of  $\bar{K}NN - \pi\Sigma N$  system were performed to define the binding energy and width of  $K^-pp$  system. The efficiency of the so called HSE method was investigated. We have calculated the transition probability (11) for  $(Y_K)_{I=0} + N \rightarrow \pi\Sigma N$  reaction in the energy region between the  $\bar{K}NN$  and  $\pi\Sigma N$  thresholds. We have ex-

amined how the signature of the  $K^-pp$  quasi-bound state in the three-body  $\bar{K}NN - \pi\Sigma N$  system manifests itself in the transition probabilities on the real energy axis. To investigate the dependence of the resulting transition probabilities on models of  $\bar{K}N - \pi\Sigma$  interaction, several versions of  $\bar{K}N - \pi\Sigma$  potentials, which can produce different structures for  $\Lambda(1405)$  resonance, were used. Within this model, we have found a bump produced by  $\bar{K}NN - \pi\Sigma N$  system appearing in the  $(Y_K)_{I=0} + N \rightarrow \pi\Sigma N$  transition probabilities in the energy region around the  $\bar{K}NN - \pi\Sigma N$  pole position. We found, that we can find a distinct peak in the mass spectrum for momentum  $p_N = 100 - 250$  MeV/c. In the present calculations, we also found that the shape and position of the peaks in the transition probability are independent of the momentum  $p_N$  of the initial  $(Y_K) + N$  channel. Therefore, this fact implies that the bumps are corresponding to the  $\Lambda(1405)$  and  $K^-pp$  quasi-bound states. Since, the nucleon in the initial state covers a continuous, we should include the effect of all momenta in transition amplitude. We calculated the averaged transition probability  $(Y_K)_{I=0} + N \rightarrow \pi\Sigma N$ . Furthermore, we have shown that not only we can see the signature of the  $K^-pp$  quasi-bound state, but also, we can see the effect of the branch points in the Faddeev amplitudes (complex plane) and transition probabilities which are resulting from  $\Lambda(1405)$  pole. we have shown that the bump structures related to the the branch points can affect the peak corresponding to the  $K^-pp$  quasi-bound state. Thus, in the mesonic decay channel, we should consider the effect of the branch points and this reaction would also be helpful to reveal the dynamical origin of  $\Lambda(1405)$  resonance.

- 
- [1] Y. Akaishi and T. Yamazaki, Phys. Rev. C, 2002, **65**: 044005.
  - [2] T. Yamazaki and Y. Akaishi, Phys. Lett. B, 2002, **535**: 70.
  - [3] A. Dote, H. Horiuchi, Y. Akaishi and T. Yamazaki, Phys. Lett. B, 2004, **590**: 51.
  - [4] A. Dote, H. Horiuchi, Y. Akaishi and T. Yamazaki, Phys. Rev. C, 2004, **70**: 044313.
  - [5] N. V. Shevchenko, A. Gal and J. Mares, Phys. Rev. Lett., 2007, **98**: 082301.
  - [6] N. V. Shevchenko, A. Gal, J. Mares and J. Revai, Phys. Rev. C, 2007, **76**: 044004.
  - [7] Y. Ikeda and T. Sato, Phys. Rev. C, 2007, **76**: 035203.
  - [8] Y. Ikeda and T. Sato, Phys. Rev. C, 2009, **79**: 035201.
  - [9] A. Dote, T. Hyodo and W. Weise, Nucl. Phys. A, 2008, **804**: 197.
  - [10] A. Dote, T. Hyodo and W. Weise, Phys. Rev. C, 2009, **79**: 014003.

- [11] Y. Ikeda, H. Kamano and T. Sato, Prog. Theor. Phys., 2010, **124**: 533.
- [12] S. Marri and S. Z. Kalantari, Eur. Phys. J. A, 2016, **52**: 282, arXiv:1611.09025 [nucl-th].
- [13] S. Marri, S. Z. Kalantari and J. Esmaili, Eur. Phys. J. A, 2016, **52**: 361, arXiv:1612.00685 [nucl-th].
- [14] S. Marri and J. Esmaili, arXiv:1902.00903 [nucl-th].
- [15] S. Maeda, Y. Akaishi and T. Yamazaki, Proc. Jpn. Acad., Ser. B, 2013, **89**: 418.
- [16] T. Koike and T. Harada, Phys. Lett. B, 2007, **652**: 262.
- [17] T. Yamazaki *et al.*, Phys. Rev. Lett., 2010, **104**: 132502.
- [18] T. Yamazaki and Y. Akaishi, Proc. Jpn. Acad., Ser. B, 2007, **83**: 144.
- [19] T. Yamazaki and Y. Akaishi, Phys. Rev. C, 2007, **76**: 045201.
- [20] T. Nagae., J-PARC proposal E27; Y. Ichikawa *et al.*, Prog. Theor. Exp. Phys., 2015, 021D01.
- [21] M. Iwasaki, *et al.*, J-PARC E15 proposal; T. Hiraiwa *et al.*, Int. J. Mod. Phys. A, 2011, **26**: 561.
- [22] T. Koike and T. Harada, Phys. Rev. C, 2009, **80**: 055208.
- [23] J. Yamagata-Sekihara, D. Jido, H. Nagahiro, and S. Hirenzaki, Phys. Rev. C, 2009, **80**: 045204.
- [24] S. Ohnishi, Y. Ikeda, H. Kamano and T. Sato, Phys. Rev. C, 2013, **88**: 025204.
- [25] T. Sekihara, E. Oset and A. Ramos, Prog. Theor. Exp. Phys. 2016, **2016**: 123D03, [arXiv:1607.02058 [hep-ph]].
- [26] T. Sekihara, E. Oset and A. Ramos, JPS Conf. Proc. 2017, **13**: 020002, [arXiv:1611.07361 [nucl-th]].
- [27] T. Sekihara, E. Oset and A. Ramos, Acta Phys. Polon. B 2017, **48**: 1869, [arXiv:1709.08487 [nucl-th]].
- [28] N. V. Shevchenko, Phys. Rev. C, 2012, **85**: 034001.
- [29] N. V. Shevchenko, Nucl. Phys. A, 2012, **890-891**: 50.
- [30] E. O. Alt, P. Grassberger, and W. Sandhas, Phys. Rev. C, 1970, **1**: 85.
- [31] J. Revai, Few-Body Syst., 2013, **54**: 1865.
- [32] P. Grassberger, W. Sandhas, Nucl. Phys. B, 1967, **2**: 181.
- [33] I. M. Nadrodetsky, Nucl. Phys. A, 1974, **221**: 191.
- [34] A. C. Fonseca, L. Streit, Lect. Notes Phys., 1986, **273**: 161.
- [35] A. Fix and H. Arenhovel, Phys. Rev. C, 2002, **66**: 024002.
- [36] S. B. Carr, I. R. Afnan and B. F. Gibson, Phys. Rev. C, 1998, **57**: 2858.
- [37] R. Dalitz and S. Tuan, Phys. Rev. Lett. 1959, **2**: 425.
- [38] J. Oller and U. G. Meissner, Phys. Lett. B 2001, **500**: 263.
- [39] T. Hyodo and W. Weise, Phys. Rev. C 2008, **77**: 035204.
- [40] D. Jido, J. Oller, E. Oset, A. Ramos, and U. Meissner, Nucl. Phys. A 2003, **725**: 181.

- [41] A. Cieply, M. Mai, U. G. Meissner and J. Smejkal, arXiv:1603.02531 [hep-ph].
- [42] K. P. Khemchandani<sup>1a</sup>, A. Martnez Torres, and J. A. Oller, arXiv:1810.09990 [hep-ph].
- [43] A. Feijoo, V. Magas and A. Ramos, arXiv:1810.07600 [hep-ph].
- [44] K. Miyahara, T. Hyodo and W. Weise, Phys. Rev. C 2018, **98**: 025201.
- [45] M. Bazzi *et al.*, (SIDDHARTA collaboration), Phys. Lett. B, 2011, **704**: 113.
- [46] M. Iwasaki, *et al.*, Phys. Rev. Lett., 1997, **78**: 3067.
- [47] T. M. Ito *et al.*, Phys. Rev. C, 1998, **58**: 2366.
- [48] A. Gal and H. Garcilazo, Nucl. Phys. A, 2014, **928**: 73.
- [49] H. Zankel, W. Plessas and J. Haidenbauer, Phys. Rev. C, 1983, **28**: 538.
- [50] M. Torres, R. H. Dalitz, and A. Deloff, Phys. Lett. B, 1986, **174**: 213.
- [51] L. Schlessinger, Phys. Rev., 1968, **167**: 1411.
- [52] H. Kamada, Y. Koike, and W. Gloeckle, Prog. Theor. Phys., 2003, **109**: 869.